INTERNATIONAL JOURNAL OF SUSTAINABLE CONSTRUCTION ENGINEERING AND TECHNOLOGY
VOL. 13 NO. 1 (2022) 185-201

IJSCET

http://publisher.uthm.edu.my/ojs/index.php/ijscet

ISSN : 2180-3242 e-ISSN : 2600-7959

International Journal of Sustainable Construction Engineering and Technology

Evaluation of Indonesia's Conventional Track Performance Based on Mechanistic Approach

Dian M. Setiawan[1*]

[1]Department of Civil Engineering,
Universitas Muhammadiyah Yogyakarta Jl. Brawijaya, Bantul, 55813, INDONESIA

*Corresponding Author

DOI: https://doi.org/10.30880/ijscet.2022.13.01.017
Received 13 March 2022; Accepted 21 March 2022; Available online 16 May 2022

Abstract: Most railway track dynamics models focus on the high-speed train. However, freight trains non only have strong implications for track dynamics, but also the response of conventional track subjected to the low speed of freight train models are rarely published. This paper developed a 2-Dimensional conventional railway track model based on the multipurpose finite element package Abaqus/CAE, which considers four structure layers: sleepers, ballast, sub-ballast, and subgrade subjected to three different freight train speeds (very low, low, and normal) and two different freight train axle loads (normal, 18,000 kg, and heavier, 27,000 kg). The most obvious finding to emerge from this study is that running the long-chain coal "Babaranjang" freight train with 70 km/h of operating speed and 27,000 kg of axle load is suggested to increase the hauling capacity of the Babaranjang train and at the same time to ensure the safety of its operation. Also, the present study confirms previous findings and contributes additional evidence that a train with a very low operation speed could deteriorate the conventional track structure, and it will be worsened when this type of train is operated with a higher axle load.

Keywords: Conventional track, compressive stress, cyclic loading, deformation, elastic modulus, mechanistic

1. Introduction

Most of the Indonesia's railway networks are currently relics of the Dutch Government's era and desperately need special and intensive handling because of technological and other changes (Dwiatmoko et al., 2020). The importance of rail track structure performance in Indonesia related to the track quality was studied by Setiawan and Rosyidi (2016) and Setiawan (2016). Indonesia's conventional track component is damaged more frequently, leading to a threat of running safety due to the running of heavy haul trains. However, maintaining Indonesia's conventional railway tracks is costly and difficult to manage effectively. The rail track maintenance stakeholders in the Indonesian railway system always experience difficulties finding the proper window time for the maintenance work.

Some typical problems of Indonesia's conventional track system are presented in Fig 1. Indonesia's conventional track experienced ballast deformations and track misalignments. Also, it was easy to find the track sections with ballast material deficiency. Although the design speed of the curve track section in Indonesia's conventional track is between 90 to 120 km/hour, however, in practice, the train is only permitted to run between 45 to 70 km/hour. Fig. 1 also shows several black spots in the curve track section where the train derailments occur, and some wheel trains' footprints and broken concrete sleepers can be found after the occurrence of train derailments.

Several studies have been reported to enhance the durability of the ballast layer in the conventional track structure. Sol-Sanchez et al. (2014), Sol -Sanchez et al. (2015), Signes et al. (2016), Indraratna et al. (2017), Navaratnarajah et al. (2017), Setiawan and Rosyidi (2018), Setiawan and Rosyidi (2019), and Setiawan et al. (2019) considered and utilized

*Corresponding author: diansetiawanm@ft.umy.ac.id

the rubber materials in the form of crumb rubber from used tires or rubber mats as an alternative solution to improve deformation performance and degradation behavior of ballast layer in the conventional track structure. However, rubber material properties are not resistant to temperature heating because it is categorized as a thermoplastic material (Hameed and Shashikala, 2016).

a b

Fig. 1 - Some examples of black spots in Indonesia's conventional track line: (a) lack of ballast materials; (b) broken concrete sleepers after train derailments

Analyzing conventional track material specification and calculating its thickness requirements using the European' empirical approach was performed by Setiawan et al. (2013). In designing Indonesia's conventional track and determining its layer thicknesses, rail track engineers need to look at the Minister of Transportation Regulation No. 60 of 2012 (Sekretariat, 2012) concerning Technical Requirements for Rail Track. However, this regulation was also developed using empirical performance concepts related to train traffic and maximum train speed, as shown in Table 1.

Table 1 - Classification of Indonesia's conventional track based on the passing tonnage per year for narrow gauge 1067 mm (Sekretariat, 2012)

Rail track class	Passing tonnage (Tons/Year)	Design speed (Km/Hour)	Axle load (Tons)	Rail type	Sleeper type Distance between sleeper (mm)	Ballast thickness (mm)
I	$> 20.10^6$	120		R.60/R.54	Concrete 600	300
II	10.10^6 - 20.10^6	110		R.54/R.50	Concrete/Wooden 600	300
III	5.10^6 - 10.10^6	100	18	R.54/R.50/R.42	Concrete/Wooden 600	300
IV	$2.5.10^6$ - 5.10^6	90		R.54/R.50/R.42	Concrete/Wooden 600	250
V	$< 2.5.10^6$	80		R.42	Wooden/Steel 600	250

As Table 1 shows, Indonesia's railway regulator is classifying their conventional track systems only based on the estimation of passing tonnage per year. For example, if the predicted passing tonnage is more than twenty million tons/year, the new conventional track should be built with a design speed of 120 km/h, axle loads 18 tons, concrete sleepers, and ballast thickness 300 mm. However, this approach has several significant limitations regarding validity. First, the method only considers a single axle load, 18 tons. Secondly, this approach was established and developed only based on specific construction technology and only for the conventional track. In addition, the mechanistic performance of structural components was not considered in this regulation which is crucial in ensuring the optimum structural materials properties and layer thicknesses. Lastly, the design period was not accounted for, so we can assume that Indonesia's conventional track design method has uncertainty issues regarding structural service life.

Based on the Indonesian' empirical approach limitations, one of the most straightforward efforts to solve these problems is developing the mechanistic-empirical design concept. One of the advantages of the mechanistic-empirical method is the concept that considers the variations in moisture and temperature on the mechanical properties of the conventional track layers and its ability to estimate structural service life. Moreover, in the mechanistic-empirical approach, there are more structural performance (failure) criteria in the design process: the vertical compressive stress at the top of the subgrade layer.

Some studies have been published to predict the performance of ballasted rail tracks considering the mechanistic-empirical design concept using the KENTRACK program (Liu, 2013; Lemma, 2016). Soto et al. (2017) and Soto and Di Mino (2017) analyzed and designed the railway track-beds subjected to long-distance intercity Italian train configuration with a static load of 16 tons per axle. Setiawan (2021) and Setiawan (2022) conducted the mechanistic-empirical approach in analyzing the performance of Indonesia' conventional track subjected to long-chain coal "Babaranjang" freight train loading using KENTRACK software to calculate the compressive stresses at the top of the subgrade layer and at the same time predict the service life of subgrade layer.

However, the mechanistic part of the KENTRACK software is limited in determining the mechanical response of rail track structures based on a multi-layer system. In addition, the accurate prediction of distresses in rail track structures is limited in the approach considering the nature of transfer function and the statistical calibration process. Therefore, more work needs to be done to construct the mechanistic modeling approach a more practical method and make the process efficient by accounting for a large number of traffic loads while maintaining reasonable computing time and costs (Rahmani et al., 2020).

Several studies have been accomplished to evaluate the response of conventional rail tracks considering the full-mechanistic approach. Most of them focus on the effect of high-speed train operation on the ballasted rail track performance. Wang and Zeng (2004) and Zeng (2005) present the 2-Dimensional numerical simulation of a high-speed track foundation subjected to dynamic loading with different materials used as track-bed underlayment materials. Fang et al. (2011) performed a numerical analysis using a finite element program to compare the dynamic behaviors of several types of track-bed structures. Prakoso (2012) presented 2-Dimensional models of railway superstructures and discussed the basic theories behind the advanced rail track modeling using the finite element method.

To describe the dynamic load distribution of a high-speed train, Shih et al. (2014) developed a 3-Dimensional time-domain approach of the rail track model. The results allow the vibration of the whole system to be evaluated and the critical speed to be established. Shih et al. (2016) conducted systematic research to compare different boundary conditions, different models of soil damping, and different sizes and shapes of finite element mesh to develop guidance in selecting appropriate finite element models for moving load problems. Varandas et al. (2016) numerically analyzed the stress changes in the ballast due to the train passages considering the 3-Dimensional model of the track-ballast-soil system using the finite element method.

A sophisticated 3-Dimensional finite elements modeling was developed by Sayeed and Shahin (2016) to investigate the impact of train speed on the dynamic response of the track-ground system as well as some factors of the track-ground system affecting the critical speed, including the modulus and thickness of conventional track materials and the amplitude of train loading. With the aid of numerical modeling, Wehbi and Musgrave (2017) studied the optimum value for conventional track stiffness for the United Kingdom's railways to facilitate the efficient and effective design and maintenance. Wu et al. (2019) developed a 3-Dimensional railway track dynamics model that considers four structures layers: rails, sleepers, ballast, and sub-ballast.

Babaranjang train, shown in Fig. 2, is the heaviest and the longest train in Indonesia's railway system with 18 tons axle loads and is operated along the South Sumatera and Lampung Province rail track line. Its operation is crucial in fulfilling the energy needs of Indonesia's industry. According to Hardian (2011), Indonesia has 105 billion tons of coal resources, where 45% of the total resources are available in the South Sumatra. Unfortunately, due to the lack of Indonesia's conventional track capability, especially in the South Sumatera region, the maximum axle load is only 18,000 kg, which is significantly lower compared to other countries that can run the freight train with a maximum axle load of up to 27,000 kg and 36,000 kg. Therefore, one solution to optimize and maximize the coal-hauling capacity in Indonesia, as the train operator, PT. KAI runs the Babaranjang train (Long Chain Coal Train) with more than 50 cars. Each car has approximately 22.5 meters in length. It means that the total length of one set Babaranjang train is 1125 meters.

Fig. 2 - Babaranjang (long chain coal) train in South Sumatera, Indonesia

However, this condition led to several problems. First, the train operation system in South Sumatera and Lampung rail track lines becomes more complicated due to the existence of a mix of traffic between the long-chain coal Babaranjang freight train consisting of 50 carriages and the passenger train that only consist of 8 carriages. Also, the operation of the Babaranjang train causes complaints from road users because they have to wait in line at the level crossing with a long waiting time, which is around 10 minutes each time the Babaranjang train passes the level crossing between the rail and highway. Therefore, by increasing the axle load of the Babaranjang train from 18,000 kg to 27,000 kg, it will have a positive impact on increasing the carrying capacity of the Babaranjang train and, at the same time, reducing the length of the Babaranjang train series by up to 50%. Unfortunately, until now, no research has been conducted to evaluate the impact of increasing the axle load of the Babaranjang train on the performance of Indonesia's conventional railroads in South Sumatra.

On another side, although the conventional track for the Babaranjang train was constructed with the design speed of 120 km/h, however in practice, the Babaranjang train is only permitted to run with an operational speed between 45 km/h to 70 km/h because of the existence of black spots with a high risk of derailments due to large deformation of the track. Unfortunately, no scientific study has been performed to analyze the response of Indonesia's conventional track under a very low operational speed to minimize the risk of the train derailment. Therefore, this paper focus on the full-mechanistic approach in assessing the performance of Indonesia’s conventional track subjected to different operating speed and various axle loads of Babaranjang (Long Chain Coal) freight train to accurately capture and predict Indonesia’ conventional track performances and responses. This study will help Indonesia's railway stakeholders decide the appropriate solution for the Babaranjang train operation's safety and loading capacity.

2. Research Method

2.1 Geometric and Dimension of Rail Track

Table 2 presents the thickness of Indonesia's conventional track evaluated in this study, a typical dimension for the rail track 1st Class. Fig 3 illustrates the geometry and dimension of Indonesia's conventional track. The measurements positions of strain-stress and displacement are also shown in Fig 3.

Table 2 - Geometric and dimension of conventional track

Conventional track layer	Thickness (mm)
Ballast	300
Sub-Ballast	400
Subgrade	3300
Total	**4000**

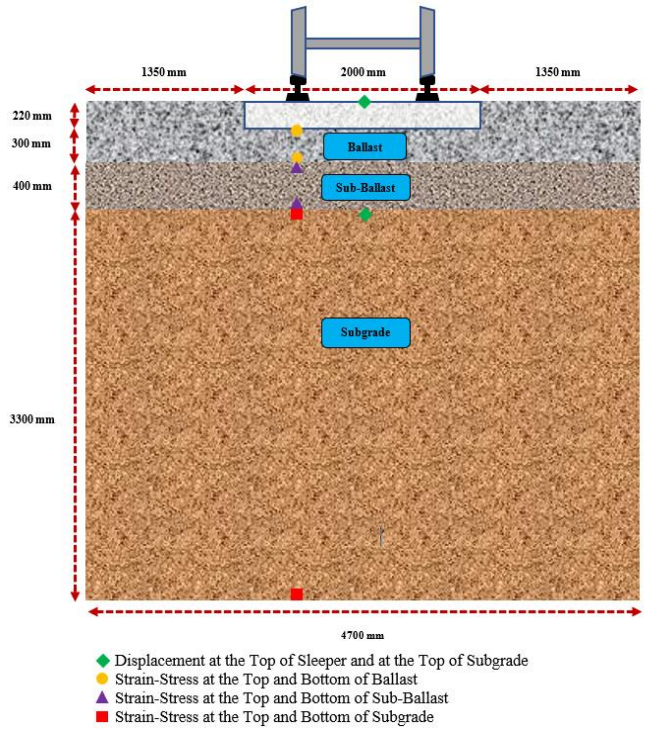

Fig. 3 - 2D sketch and measurement position

2.2 Material Properties

All materials in the conventional track evaluated in this study are considered to have a linear elastic behavior. The materials parameters are the Elastic Modulus, Poisson's Ratio, and Mass Density. Material inputs for the simulation of Indonesia's conventional track are shown in Table 3.

Table 3 – Material properties

Conventional track layer	Elastic modulus E (MPa)	Poisson's ratio ν	Mass density ρ (kg/m^3)
Sleeper (Lee et al., 2018)	29100	0.30	2300
Ballast (Hassan et al., 2020)	130	0.20	1900
Sub-Ballast (Hassan et al., 2020)	120	0.30	1900
Subgrade (Lee et al., 2018)	80	0.30	2000

2.3 Cyclic Loading

As Table 4 presents, three different train operating speeds were considered in this study, which is 45 km/h to represent very low train speed during extreme train speed restriction conditions (Case 1), 70 km/h to represent low train speed during normal train speed restriction condition (Case 2), and 120 km/h to represent normal (design) train speed without train speed restriction condition (Case 3). Each case will be assigned for two different axle loads, 18,000 kg (Case 1A, 2A, and 3A) to represent normal Babaranjang train loading, and 27,000 kg (Case 1B, 2B, and 3B) to represent heavier Babaranjang train loading.

Table 4 – Case studied

Train speed (km/h)	Axle load (kg)	Case
45 km/h	18,000	1A
	27,000	1B
70 km/h	18,000	2A
	27,000	2B
120 km/h	18,000	3A
	27,000	3B

The dynamic wheel load was computed using Eq. 1 and Eq. 2, according to Talbot Formula (Rosyidi, 2015).

$$I_p = 1 + 0.01\left(\frac{V}{1.609} - 5\right) \quad (1)$$

$$P_d = P_s \times I_p \quad (2)$$

Where I_p is conversion factor, V is design speed in km/hour, P_s is static wheel load of a train in kg, and P_d is dynamic wheel load of a train also in kg.

In order to compute the dynamic wheel load of Babaranjang train, parameters V are used, for example, 45 km/hr with a static wheel load of 9000 kg (axle load of 18,000 kg) or 88.3 kN; then, the dynamic wheel load for the Babaranjang train is 11,067 kg or 109 kN (please see Table 5). The loading frequency of approximately 0.7 Hz was determined using Eq. 3 based on the speed V of 45 km/h and distance between the axis of two bogies of the train (L_b), 17.733 m (please see Fig. 4).

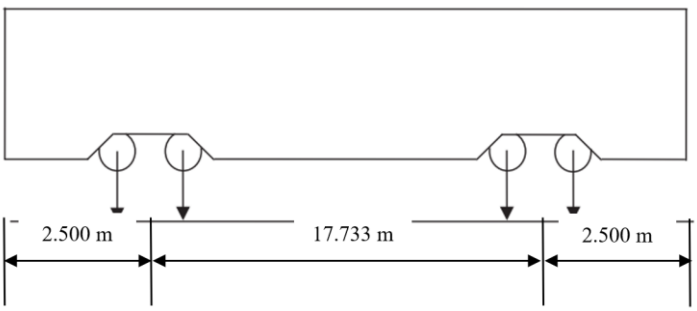

Fig. 4 - Distance between two bogies (L_b) (Wang et al., 2020)

$$f_b = \frac{V}{L_h} = \frac{45\ {}^{km}/_{h}}{17.733\ m} = \frac{45{,}000\ {}^{m}/_{3600\ s}}{17.733\ m} = 0.7\ \frac{1}{s} = 0.7\ Hz \tag{3}$$

Therefore, the cyclic loading was applied with the maximum load 11,067 kg or 109 kN, frequency 0.7 Hz, and 20,000 loading cycles, while the total loading time (time period) is 20,000 cycles/0.7 Hz = 28,373 seconds, as shown in Table 5.

Fig. 5 shows the cyclic loading configuration for all cases in this study.

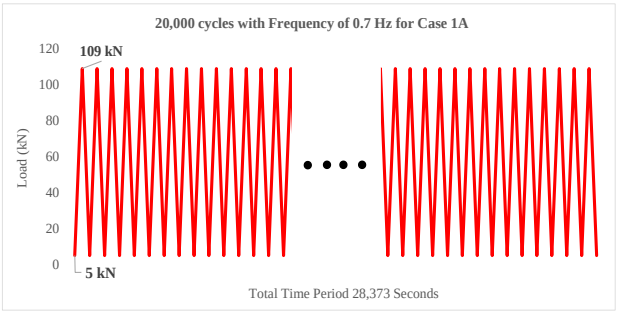

(a) Case 1A (45 km/h, 18,000 kg)

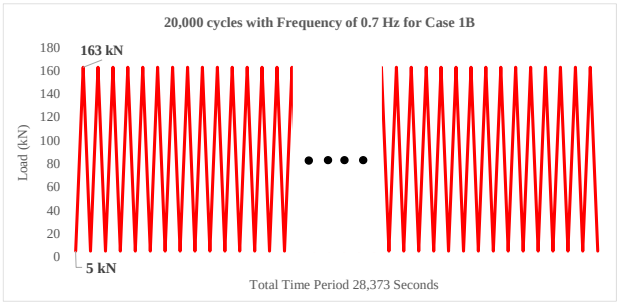

(b) Case 1B (45 km/h, 27,000 kg)

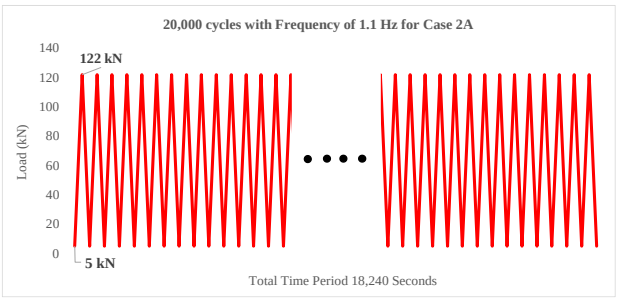

(c) Case 2A (70 km/h, 18,000 kg)

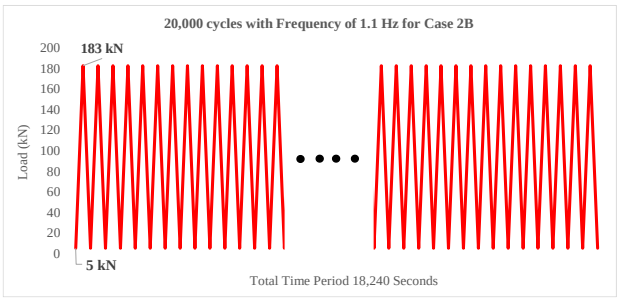

(d) Case 2B (70 km/h, 27,000 kg)

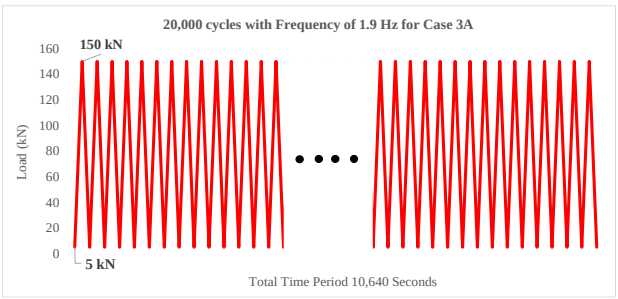

(e) Case 3A (120 km/h, 18,000 kg)

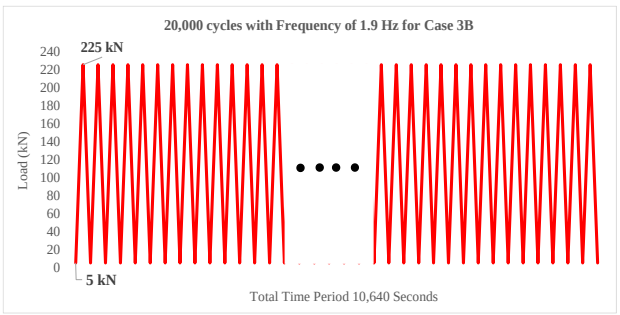

(f) Case 3B (120 km, 27,000 kg)

Fig. 5 - Cyclic loading configuration

Table 5 – Simulated cyclic load

Train speed (km/h)	Axle load (kg)	Static wheel load (kg)	Dynamic load (kg)	Dynamic load (kN)	Bogie passage frequency (Hz)	Loading cycles	Total time period (s)
45 km/h	18,000	9,000	11,067	109	0.7	20,000	28,373
	27,000	13,500	16,601	163			
70 km/h	18,000	9,000	12,465	122	1.1	20,000	18,240
	27,000	13,500	18,698	183			
120 km/h	18,000	9,000	15,262	150	1.9	20,000	10,640
	27,000	13,500	22,893	225			

2.4 Mechanistic Approach

The 2-dimensional (2D) numerical simulation was performed based on Abaqus/CAE's multipurpose finite element package to compare the measurement results. The simulation model of the conventional track was sketched as in Fig. 3,

and the 2D mesh was presented in Fig. 6. The suitable mesh was determined for predicting conventional track response under cyclic loading. The mesh 55 by 50 mm was used in the sleeper, and the mesh 50 by 50 mm was used in the ballast, sub-ballast, and subgrade, respectively.

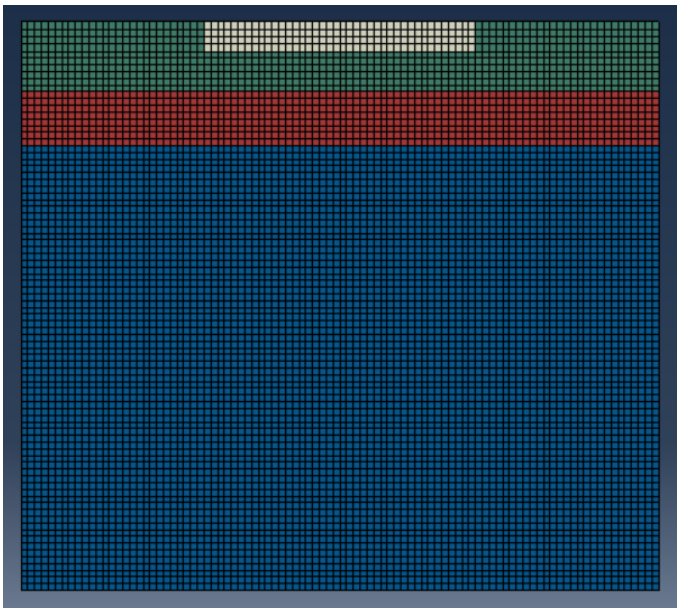

Fig. 6 - The 2-dimensional meshing

Material inputs for the conventional track simulation are shown in Table 3. The material properties of the sleeper and subgrade were adopted from Lee et al. (2018). At the same time, the material properties of the ballast and sub-ballast were adopted from Hassan et al. (2020). In this analysis, the interactions between layers were assumed to be fully bonded, and the boundary condition was defined as the soil box condition; hence, the horizontal displacement at the side of the model and the vertical displacement at the bottom were fixed. The sleeper was assumed to be a rigid material; hence, the deformation in the conventional track was determined by subtracting the displacement at the top of the sleeper with the displacement at the top of the subgrade. This paper has used concentrated forces to simplify wheel-rail contact forces. Therefore, the wheel-rail contact, and vehicle system dynamics have been neglected.

3. Results and Discussions

3.1 Stress-Strain Component

This section presents the vertical strain distribution, horizontal strain distribution, and the evaluation of strain-stress (σ-ε) component in several locations inside the ballast, sub-ballast, and subgrade layer, as illustrated in Fig 7, Fig. 8, and Fig. 9, respectively.

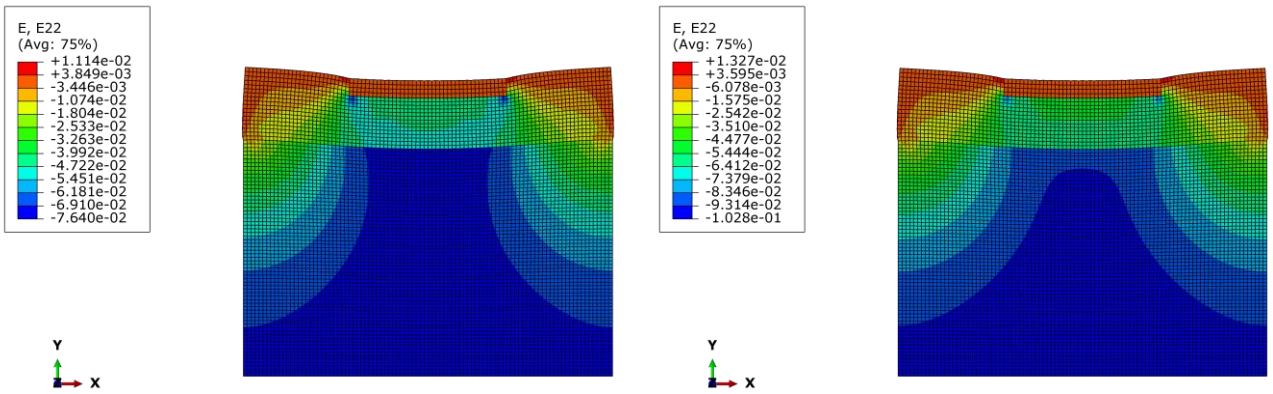

(a) Case 1A (45 km/h, 18,000 kg)

(b) Case 1B (45 km/h, 27,000 kg)

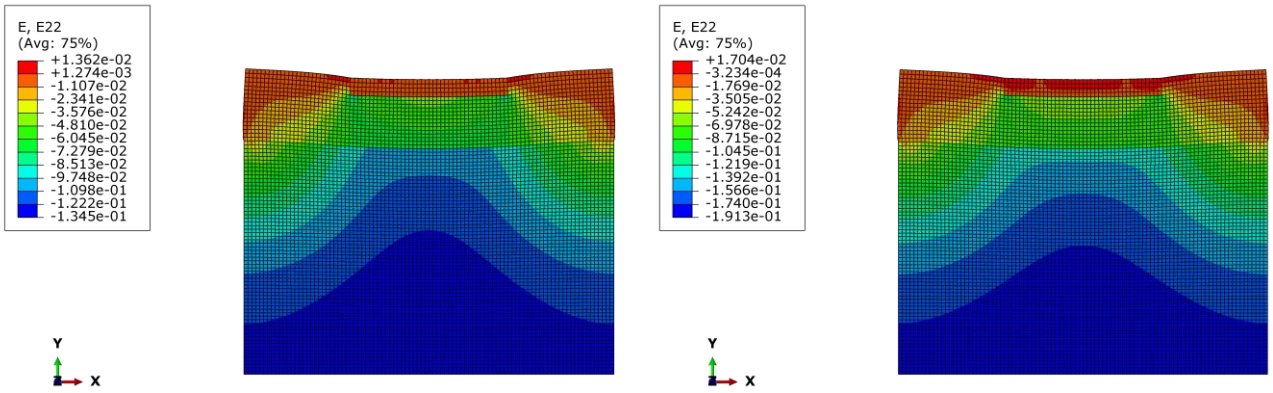

(c) Case 2A (70 km/h, 18,000 kg) (d) Case 2B (70 km/h, 27,000 kg)

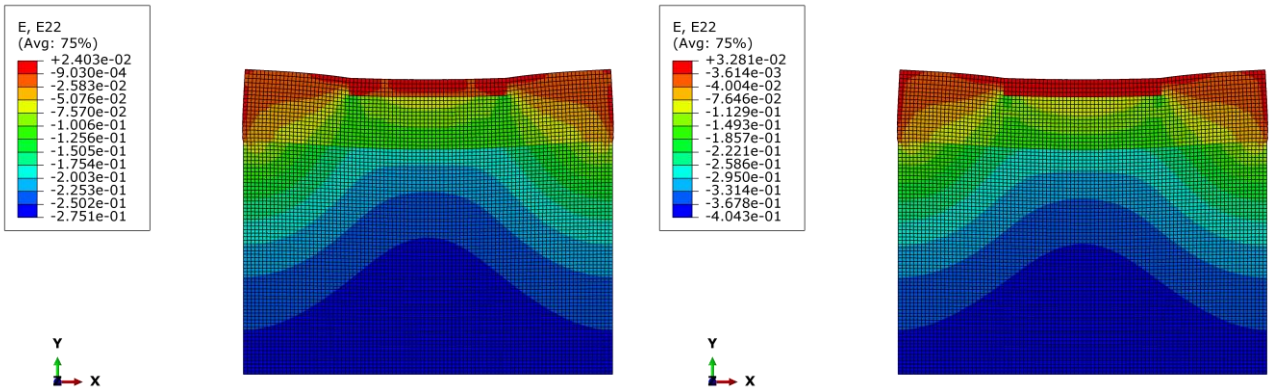

(e) Case 3A (120 km/h, 18,000 kg) (f) Case 3B (120 km, 27,000 kg)

Fig. 7 - Vertical strain distribution

As Fig. 7 shows, the vertical strain development inside the structure as the loading reaches twenty thousand times. As expected, increasing the train speed (please see and compare Fig. 7a vs. Fig 7c vs. Fig 7e) and axle load (please see and compare Fig. 7b vs. Fig 7d vs. Fig 7f) will increase the vertical strain below the sleeper. Surprisingly, the change in the vertical strain below the sleeper in Case 1 (at very low speed, 45 km/h) due to the increasing of axle load (Fig. 7a vs. Fig 7b) is more significant than in Case 2 (at low speed, 70 km/h) (please see and compare Fig. 7c vs. Fig 7d) and in Case 3 (at normal speed, 120 km/h) (please see and compare Fig. 7e vs. Fig 7f).

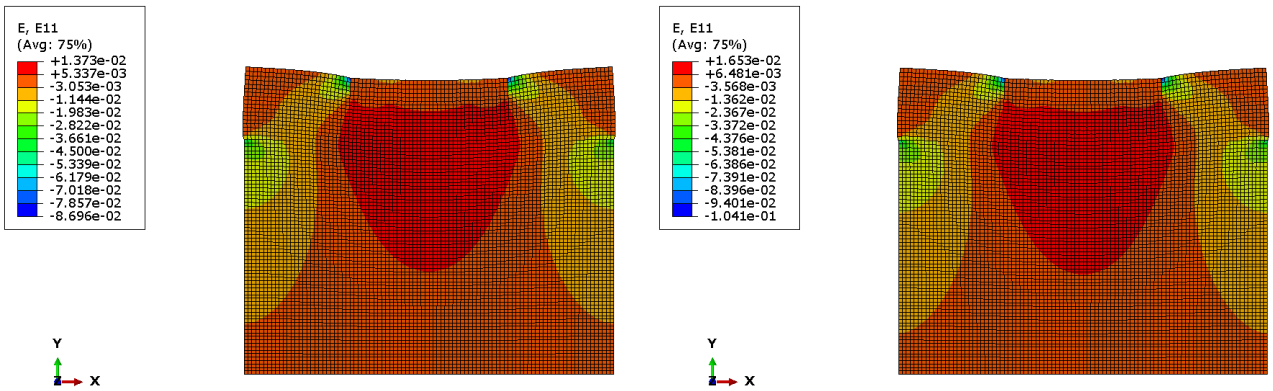

(a) Case 1A (45 km/h, 18,000 kg) (b) Case 1B (45 km/h, 27,000 kg)

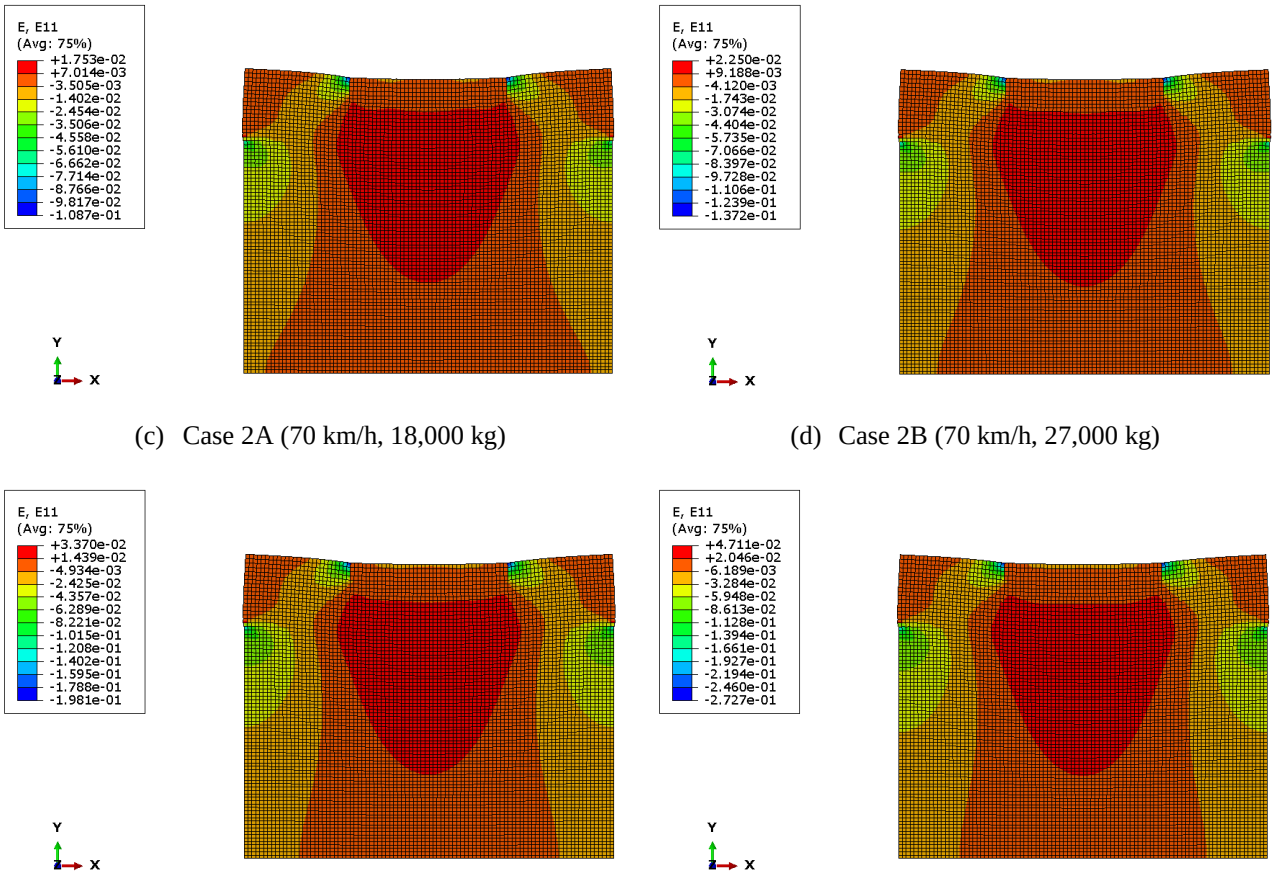

(c) Case 2A (70 km/h, 18,000 kg)

(d) Case 2B (70 km/h, 27,000 kg)

(e) Case 3A (120 km/h, 18,000 kg)

(f) Case 3B (120 km, 27,000 kg)

Fig. 8 - Horizontal strain distribution

Fig. 8 indicates the horizontal strain development inside the structure after twenty thousand loading cycles. We can conclude that increasing the axle load in the same train speed level slightly increases the development of horizontal strain below the sleeper. However, increasing the train speed (please see and compare Fig. 8a vs. Fig 8c vs. Fig 8e) and axle load (please see and compare Fig. 8b vs. Fig 8d vs. Fig 8f) will increase the horizontal strain below the sleeper significantly. In addition, we can see from Fig. 8 that there are some strain concentrations (bulb) in the edge interface between concrete sleeper and ballast and between sub-ballast and subgrade, indicating the critical area where the horizontal strain started to grow.

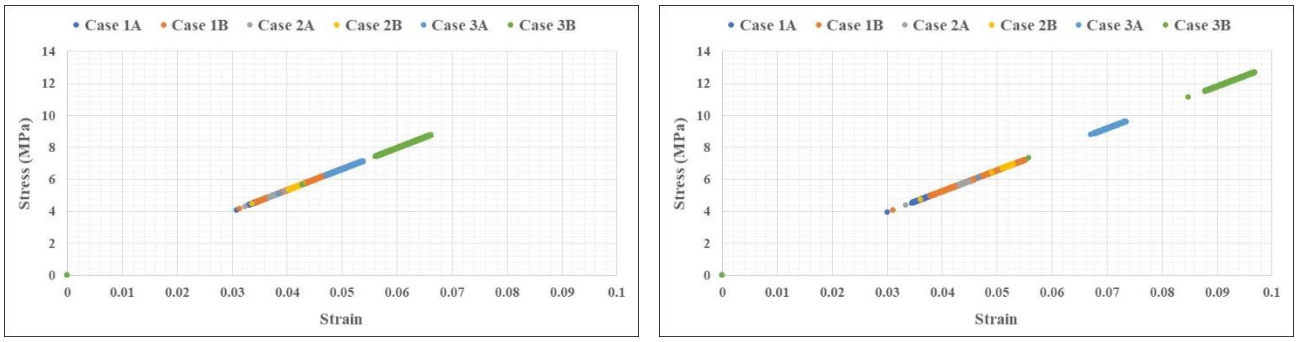

(a) Top Ballast

(b) Bottom Ballast

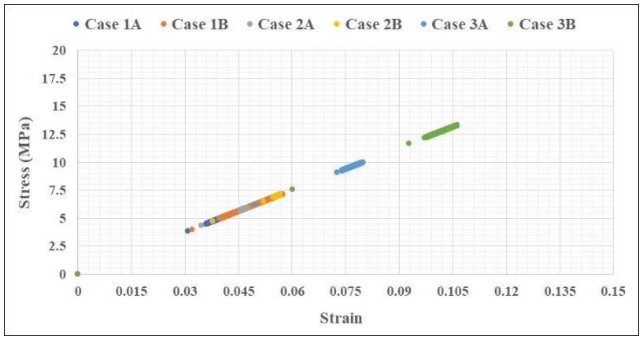

(c) Top Sub-Ballast

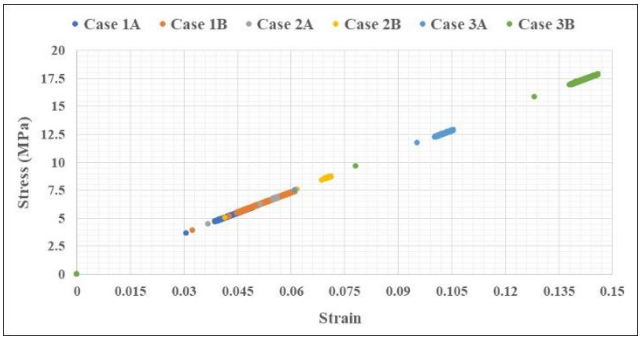

(d) Bottom Sub-Ballast

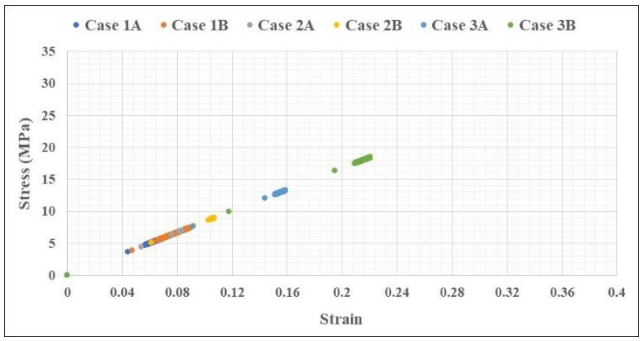

(e) Top Subgrade

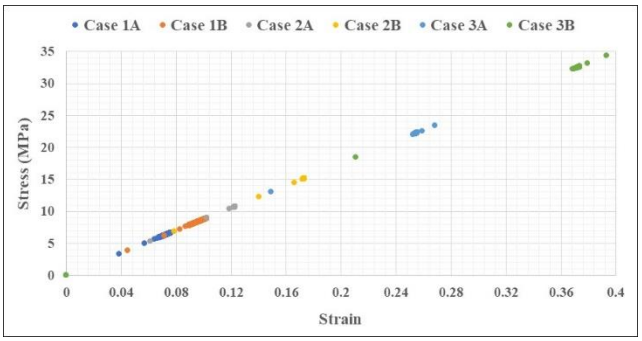

(f) Bottom Subgrade

Fig. 9 - Strain-stress component: (a) at the top of ballast layer; (b) at the bottom of ballast layer; (c) at the top of sub-ballast layer; (d) at the bottom of sub-ballast layer; (e) at the top of subgrade layer; (f) at the bottom of subgrade layer

As Fig. 9 presents, the strain-stress component for all cases is measured at the top and bottom of the ballast, sub-ballast, and subgrade layer, respectively. After twenty thousand loading cycles, the subgrade layer experiences higher stress and higher strain than the ballast and sub-ballast layers. In addition, the bottom part of the ballast, sub-ballast, and subgrade layer experience higher stress and higher strain than the top part.

The slope of the line in each graph depicted in Fig. 9 represents the measured elastic modulus. The comparison between the theoretical and the measured elastic modulus is presented in Table 6. The measured elastic modulus of the ballast, sub-ballast, and subgrade layer is slightly higher than the theoretical elastic modulus. We can conclude that, although this study used a single magnitude of theoretical elastic modulus of material for each layer, however, there is a slightly different magnitude between measured elastic modulus at the top and the bottom of each layer.

Table 6 – Theoretical elastic modulus and measured elastic modulus

Case	Layer	Theoretical elastic modulus (MPa)	Location	Measured elastic modulus (MPa)
1A	Ballast	130	Top	132.6232656
			Bottom	130.6703452
	Sub-Ballast	120	Top	124.8340926
			Bottom	121.1114120
	Subgrade	80	Top	82.8910651
			Bottom	87.2844029
1B	Ballast	130	Top	132.6304984
			Bottom	130.7337115
	Sub-Ballast	120	Top	124.9340033
			Bottom	121.3905529
	Subgrade	80	Top	83.0361342
			Bottom	87.3185345
2A	Ballast	130	Top	132.6226878
			Bottom	130.9605053
	Sub-Ballast	120	Top	125.2747270

Case	Layer	Theoretical elastic modulus (MPa)	Location	Measured elastic modulus (MPa)
			Bottom	122.2633543
	Subgrade	80	Top	83.4858202
			Bottom	87.3744536
2B	Ballast	130	Top	132.6315898
			Bottom	131.1073948
	Sub-Ballast	120	Top	125.4923012
			Bottom	122.7327731
	Subgrade	80	Top	83.7206656
			Bottom	87.4014726
3A	Ballast	130	Top	132.4100285
			Bottom	130.894133
	Sub-Ballast	120	Top	125.1352021
			Bottom	122.0860416
	Subgrade	80	Top	83.41388631
			Bottom	87.30650218
3B	Ballast	130	Top	132.3658451
			Bottom	130.9638149
	Sub-Ballast	120	Top	125.2310553
			Bottom	122.2960204
	Subgrade	80	Top	83.5200458
			Bottom	87.3504904

3.2 Measurement of Vertical Compressive Stress

Fig. 10 shows the numerical simulation results of vertical compressive stress at the top of the subgrade. As expected, the faster and the heavier Babaranjang train operation produces higher vertical compressive stress at the top of the subgrade layer. The measurement results in Table 7 for Case 1A, 1B, 2A, 2B, 3A, and 3B show vertical compressive stress values of 5.97 MPa, 6.97 MPa, 7.42 MPa, 8.94 MPa, 13.25 MPa, and 18.47 MPa, respectively, as the loading, reaches twenty thousand times. However, it is interesting to look at the results from Case 1B, where Indonesia's conventional track was modeled and subjected to a very low train speed, 45 km/h, and heavier Babaranjang train loading, 27,000 kg. From the data in Fig. 10, it is apparent that the slope of the vertical compressive stress development during twenty thousand loading cycles from Case 1B (red maroon) is higher than the other five cases.

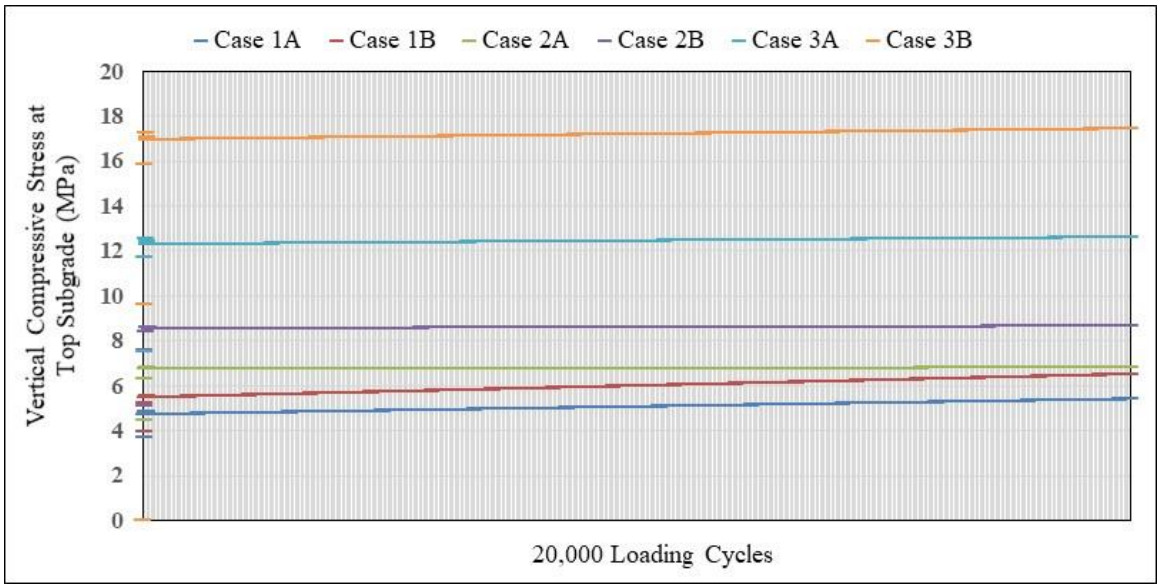

Fig. 10 - Vertical compressive stress at the top of subgrade layer

Table 7 – Vertical compressive stress (MPa) after 20,000 loading cycles and regression formula to predict vertical compressive stress after 500,000 loading cycles

Case	Vertical compressive stress (MPa) after 20,000 loading cycles	Regression formula	Predicted vertical compressive stress (MPa) after 500,000 loading cycles
1A	5.97	y = 7E-05x + 4.6907	39.6907
1B	6.97	y = 1E-04x + 5.4408	55.4408
2A	7.42	y = 8E-06x + 6.6999	10.6999
2B	8.94	y = 1E-05x + 8.5005	13.5005
3A	13.25	y = 3E-05x + 12.236	27.2360
3B	18.47	y = 5E-05x + 16.885	41.8850

According to Liu (2013), Setiawan (2021), and Setiawan (2022), the value of vertical compressive stress is crucial in controlling the deformation and in predicting the subgrade service life using the mechanistic-empirical approach in KENTRACK software. The predicted vertical compressive stress after five hundred thousand long-term loading cycles is presented in Table 7, obtained from the linear regression formula. Although the vertical compression stress after twenty thousand loading cycles in Case 1A (45 km/h and 18,000 kg) and Case 1B (45 km/h and 27,000 kg) is only 5.97 MPa and 6.97 MPa, respectively, however, after five hundred thousand loading cycles, it was predicted that the vertical compressive stress magnitude in Case 1A and Case 1B would be higher than that in Case 3A (120 km/h and 18,000 kg) and Case 3B (120 km/h and 27,000 kg). It was estimated that the vertical compressive stress in Case 1A and Case 1B after five hundred thousand loading cycles is 39.6907 MPa and 55.4408 MPa, while Case 3A and Case 3B are 27.2360 MPa and 41.8850 MPa, respectively. We can conclude that a very low train speed could deteriorate the conventional track structure, and it will be worsened when the train operates with a higher axle load. Also, it can be observed that the effect of running Babaranjang train with normal axle load, 18,000 kg, and in a very low speed, 45 km/h (Case 1A) on the change in vertical compressive stress at the top subgrade is relatively the same with the effect of running Babaranjang train with heavier axle load, 27,000 kg, and in a normal speed, 120 km/h (Case 3B), after long term Babaranjang train operation (more than twenty thousand loading cycles).

3.3 Measurement of Ballast and Sub-Ballast Deformation

As stated in the previous section, the sleeper was assumed to be a rigid material; hence, the deformation in the conventional track was determined by subtracting the displacement at the top of the sleeper with the displacement at the top of the subgrade. Fig. 11 shows the numerical simulation results of the deformation of the ballast and sub-ballast layer, and Fig 12 illustrates the growth of the ballast and sub-ballast layer's deformation in each Case after twenty thousand loading cycles. Table 8 presents the regression formula obtained from the numerical simulation results, used to predict ballast and sub-ballast deformation as the loading reaches five hundred thousand times.

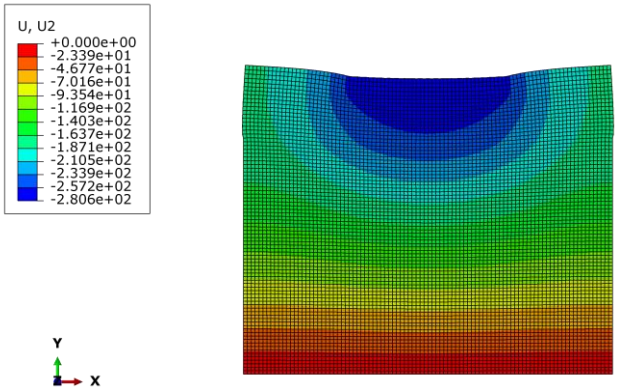

(a) Case 1A (45 km/h, 18,000 kg)

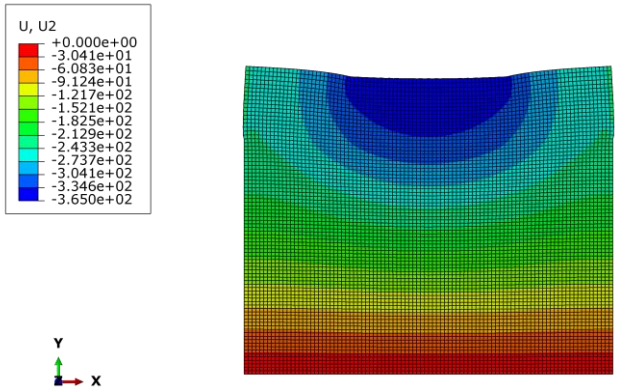

(b) Case 1B (45 km/h, 27,000 kg)

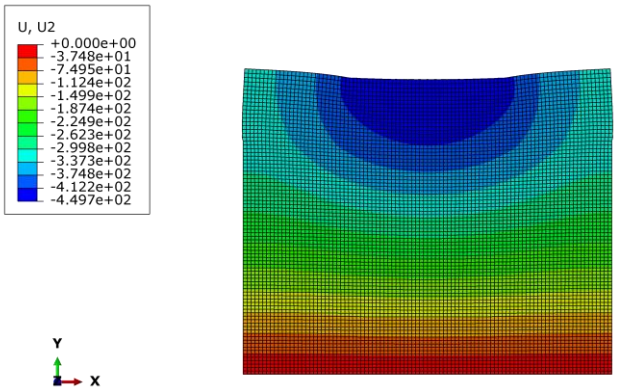

(c) Case 2A (70 km/h, 18,000 kg)

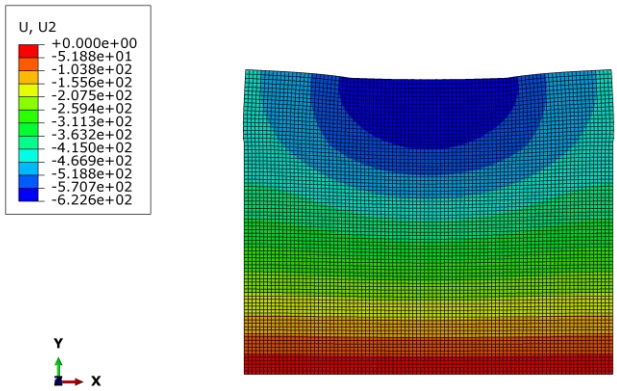

(d) Case 2B (70 km/h, 27,000 kg)

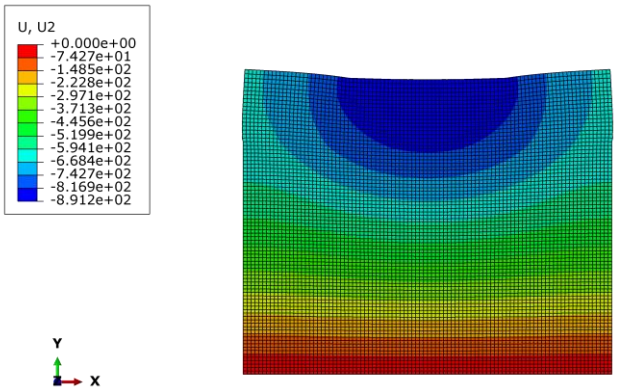

(e) Case 3A (120 km/h, 18,000 kg)

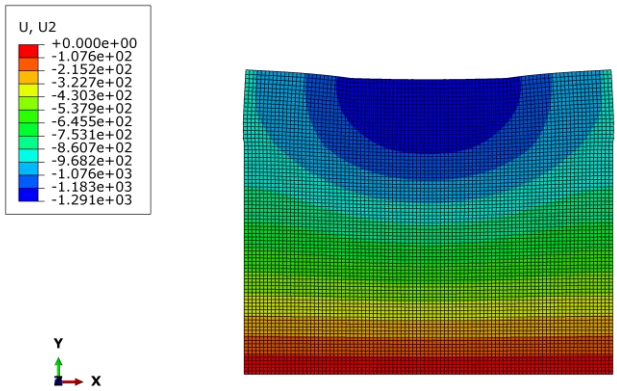

(f) Case 3B (120 km, 27,000 kg)

Fig. 11 - Numerical simulation results of ballast and sub-ballast layer's deformation

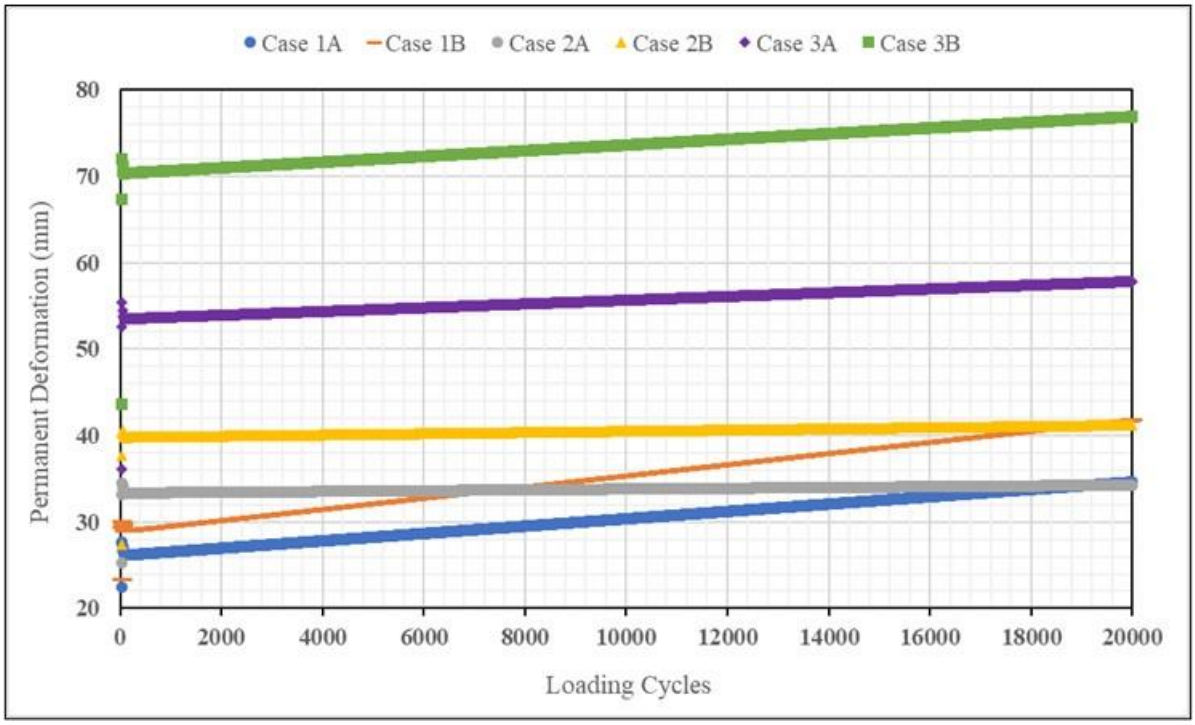

Fig. 12 - The growth of ballast and sub-ballast deformation

With a very low train speed, 45 km/h, initially, the ballast and sub-ballast deformation in Case 1A (26.056 mm) and Case 1B (28.725 mm) due to the instantaneous cyclic loading is lower than the ballast and sub-ballast deformation in Case 2A (33.252 mm) and Case 2B (39.683 mm) with the higher train speed, 70 km/h (please see Fig 12 and Table 9 column 3). However, after twenty thousand loading cycles, ballast and sub-ballast deformation in Case 1A (45 km/h, 18,000 kg) exceed ballast and sub-ballast deformation in Case 2A (70 km/h, 18,000 kg), and ballast and sub-ballast deformation in Case 1B (45 km/h, 27,000 kg) exceeds ballast and sub-ballast deformation in Case 2B (70 km/h, 27,000 kg), respectively (please see Fig 12 and Table 9 column 2). It can be evaluated from the regression formula in Table 9 column 3 that the growth of ballast and sub-ballast deformation in terms of gradient coefficient of regression formula in Case 1A and Case 1B is greater than Case 2A and Case 2B because the total time period in Case 1A and Case 1B, 28,373 seconds (please see Table 5) is significantly longer than in Case 2A and Case 2B, 18,240 seconds (please see Table 5). In other words, the conventional track in Case 1A and Case 1B experienced a longer loading process, 28,373 seconds, compared to Case 2A and Case 2B, only 18,240 seconds. We can conclude that running the train with very low speed during extreme train speed restriction conditions will worsen the conventional track structure condition. Table 9 presents the magnitude of ballast and sub-ballast deformation as the loading reaches twenty thousand times in each Case and its regression formula to predict ballast and sub-ballast deformation after significantly higher loading cycles, five hundred thousand

Table 8 – Ballast and sub-ballast deformation (mm) after 20,000 loading cycles and regression formula to predict ballast and sub-ballast deformation after 500,000 loading cycles

Case	Ballast and sub-ballast deformation (mm) after 20,000 loading cycles	Regression formula	Predicted ballast and sub-ballast deformation (mm) after 500,000 loading cycles
1A	34.61465	y = 0.0004x + 26.056	226.056
1B	41.71393	y = 0.0007x + 28.725	378.725
2A	34.26105	y = 5E-05x + 33.252	58.252
2B	41.20514	y = 8E-05x + 39.683	79.683
3A	57.81757	y = 0.0002x + 53.341	153.341
3B	76.89111	y = 0.0003x + 70.112	220.112

As expected, the ballast and sub-ballast deformation after twenty thousand loading cycles in Case 3A and Case 3B are significantly higher than the other 4 cases because of the higher train speed operated on the simulated conventional track structure. Ramos et al. (2021) also found that the stress levels and the permanent deformations are slightly amplified in the ballasted track structure under a speed of 200 km/h. The Talbot formula in Eq. 1 clearly shows that the train speed strongly influences the dynamic load of the train. With the same axle load for twenty thousand loading cycles, increasing the train speed from 70 km/h to 120 km/h or around 70% higher will increase the ballast and sub-ballast deformation up to 68% (from 34.26105 mm to 57.81757 mm) for the axle load 18,000 kg and 86% (from 41.20514 mm to 76.89111 mm) for the axle load 27,000 kg, respectively (please see Table 9 column 2). However, it is interesting to note that after five hundred thousand loading cycles, the ballast and sub-ballast deformation in Case 3A and Case 3B are 32% (153.341 mm vs. 226.056 mm) and 42% (220.112 mm vs. 378.725 mm) lower than the ballast and sub-ballast deformation in Case 1A and Case 1B, respectively (please see Table 9 column 4). Furthermore, we can conclude that the effect of running the normal axle load of Babaranjang train, 18,000 kg, in a very low speed, 45 km/h, on the ballast and sub-ballast deformation is slightly higher than the effect of running the heavier axle load of Babaranjang train, 27,000 kg, in normal speed, 120 km/h (226.056 mm in Case 1A vs. 220.112 mm in Case 3B).

A Babaranjang train set consists of 50 coal cars. Twenty thousand loading cycles in this study equal 10,000 coal carriages or the same with 200 Babaranjang train sets. Therefore, five hundred thousand loading cycles equal 250,000 coal carriages or the same with 5000 Babaranjang train sets. There are around 10 Babaranjang trains were operated per day. Therefore, we can predict that after 500 days of Babaranjang train operation, the conventional track in Case 1A, Case 1B, Case 2A, Case 2B, Case 3A, and Case 3B will experience 226.056 mm (22.606 cm), 378.725 mm (37.873 cm), 58.252 mm (5.825 cm), 79.683 mm (7.968 cm), 153.341 mm (15.334 cm), and 220.112 mm (22.011 cm) of ballast and sub-ballast deformation, respectively (please see Table 9 column 4).

4. Conclusions

This paper is focused on a parametric study and aims to evaluate the influence of very low speed, low speed, normal speed, normal axle load, and heavier axle load in the performance of the conventional track subjected to cyclic loading of freight train operations. To accomplish the proposed challenge, six numerical models in 2-Dimensional were defined. From this study, the following concluding remarks can be drawn:

1. The change in the vertical strain below the sleeper due to a very low train operation speed (45 km/h) is more significant than due to a low (70 km/h) and normal train operation speed (120 km/h). Also, increasing the axle load

in the same train speed level slightly increases the development of horizontal strain below the sleeper. However, increasing the train speed and axle load will significantly increase the horizontal strain below the sleeper.

2. Even though all material was considered linear elastic behavior where a single elastic modulus was used to represent each material's mechanical behavior in each layer, the simulation shows that the measured elastic modulus of ballast, sub-ballast, and subgrade is slightly higher than the theoretical elastic modulus. In addition, there is a difference between the elastic modulus of the layer at the top part and the elastic modulus of the layer at the bottom part. Therefore, it is worth proposing further study on the conventional track performance evaluation by considering non-linear elastic behavior (stress-dependent) of ballast, sub-ballast, and subgrade materials to better capture the performance of the conventional track structure.
3. Based on the evaluation of vertical compressive stress at the top of subgrade and the deformation of ballast and sub-ballast layer, one unanticipated finding was that a train with a very low operation speed could deteriorate the conventional track structure, and it will be worsened when this kind of train is operated with higher axle load.

Finally, several important limitations need to be considered, and further research should be explored. First, in this study, twenty thousand loading cycles are considered short-term loading conditions, and five hundred thousand loading cycles are considered long-term loading conditions, or equal to 500 days of Babaranjang train operation. Therefore, it is worth performing further study considering higher cyclic loading, which is between one million to two million loading cycles, to evaluate the longer-term performance of conventional track under various train speeds and different axle loads and considering the environmental and temperature effect. In addition, this paper has used concentrated forces with limitations in terms of the accuracy of wheel-rail forces. Therefore, further study is suggested to investigate the impact of Babaranjang train speed on the dynamic response of the vehicle-track-ground system to study the interactions between train systems and track systems in the vertical, lateral, and longitudinal direction.

Acknowledgement

The authors would like to thank the management of Universitas Muhammadiyah Yogyakarta for enabling the platform, which made for this research work possible**.**

References

Dwiatmoko, H., Suprayitno, D. & Mudjanarko, S. W. (2020). The role of railway infrastructure development on the regional economic growth. *International Journal of Sustainable Construction Engineering And Technology*, 11(1), pp. 125-135. DOI: https://doi.org/10.30880/ijscet.2020.11.01.013

Fang, M., Qiu, Y., Rose, J., West, R. & Ai, C. (2011). Comparative analysis on dynamic behavior of two HMA railway substructures. *Journal of Modern Transportation*, *19*(1), pp. 26-34. DOI: https://doi.org/10.3969/j.issn.2095-087X.2011.01.005

Hameed, A. S. & Shashikala, A. P. (2016). Suitability of rubber concrete for railway sleepers. *Perspectives in Science*, *8*, pp. 32-35. DOI: https://doi.org/10.1016/j.pisc.2016.01.011

Hardian, B. (2011). *Transport Economics of Coal Resources in South Sumatra, Indonesia*. Erasmus University Rotterdam: M.Sc. Thesis in Maritime Economics and Logistics.

Hassan, A. G., Khalil, A. A., Ramadan, I. & Metwally, K. G. (2020). Investigation of using a bituminous sub-ballast layer to enhance the structural behavior of high-speed ballasted tracks. *International Journal of GEOMATE*, *19*(75), pp. 22-132. DOI: https://doi.org/10.21660/2020.75.27822

Indraratna, B., Ngo, N. T. & Rujikiatkamjorn, C. (2017). Improved performance of ballasted rail tracks using plastics and rubber inclusions. *Procedia Engineering*, *189*, pp. 207-214. DOI: https://doi.org/10.1016/j.proeng.2017.05.033

Lee, S. H., Vo, H. V. & Park, D. W. (2018). Investigation of asphalt track behavior under cyclic loading: full-scale testing and numerical simulation. *Journal of Testing and Evaluation*.;46(3):934–942. DOI: https://doi.org/10.1520/JTE20160554

Lemma, L. (2016). *Comparative study of railway track analysis and design methods*. School of Civil and Environmental Engineering, Addis Ababa University: Master Thesis.

Liu S. (2013). *KENTRACK 4.0: A railway track-bed structural design program*. Department of Civil Engineering, University of Kentucky, USA: Theses and Dissertations.

Navaratnarajah, S. K. & Indraratna, B. (2017). Use of rubber mats to improve the deformation and degradation behavior of rail ballast under cyclic loading. *Journal of Geotechnical and Geoenvironmental Engineering*, *143*(6), pp. 1943-5606. DOI: http://doi.org/10.1061/(ASCE)GT.1943-5606.0001669

Prakoso, P. B. (2012). The basic concepts of modelling railway track systems using conventional and finite element methods. *Info Teknik*, *13*(1), pp. 57-65.

Rahmani, M., Kim, Y.R., Park, Y.B. & Jung, J. S. (2020). Mechanistic analysis of pavement damage and performance prediction based on finite element modeling with viscoelasticity and fracture of mixtures. *LHI Journal of Land, Housing, and Urban Affairs*, *11*(2), pp. 95-104. DOI: http://doi.org/10.5804/LHIJ.2020.11.2.95

Ramos, A., Correia, A. G., Calcada, R. & Alves Costa, P. (2021). Stress and permanent deformation amplification factors in subgrade induced by dynamic mechanisms in track structures. International Journal of Rail Transportation. DOI: http://dx.doi.org/10.1080/23248378.2021.1922317

Rosyidi, S. A. P. 2015. *Rekayasa Jalan Kereta Api: Tinjauan Struktur Jalan Rel*. Yogyakarta: Lembaga Penelitian, Publikasi dan Pengabdian Masyarakat Universitas Muhammadiyah Yogyakarta (LP3M-UMY).

Sánchez, M. S., Navarro, F. M. & Gamez, C. R. (2014). The use of deconstructed tires as elastic elements in railway tracks. *Materials*, *7*, pp. 5903-5919. DOI: https://doi.org/10.3390/ma7085903

Sánchez, M. S., Thom, N. H., Navarro, F. M., Gamez, C. R. & Airey, G. D. (2015). A study into the use of crumb rubber in railway ballast. *Construction and Building Materials*, *75*, pp. 19-24. DOI: https://doi.org/10.1016/j.conbuildmat.2014.10.045

Sayeed, M. A. & Shahin, M. A. (2016). Investigation into impact of train speed for behavior of ballasted railway track foundations. *Procedia Engineering*, *143*, pp. 1152-1159. DOI: http://dx.doi.org/10.1016/j.proeng.2016.06.131

Sekretariat Negara. (2012). *Peraturan Menteri Perhubungan No. 60 Tahun 2012 tentang Persyaratan Teknis Jalur Kereta Api (In English: Minister of transportation regulation no. 60 of 2012 concerning railroad technical requirements)*. Jakarta.

Setiawan, D. M. & Rosyidi, S. A. P. (2017). Track quality index as track quality assessment indicator. *Proceeding of the 19th International Symposium of Indonesian Inter-University Transportation Studies Forum (FSTPT)*, Universitas Islam Indonesia, Indonesia. Ch. 2, pp. 197-207.

Setiawan, D. M. & Rosyidi, S. A. P. (2018A). Vertical deformation and ballast abrasion characteristics of asphalt-scrap rubber track bed. *International Journal on Advanced Science, Engineering and Information Technology*, *8*(6), pp. 2479-2484. DOI: https://doi.org/10.18517/ijaseit.8.6.7411

Setiawan, D. M. & Rosyidi, S. A. P. (2019). Scrap Rubber and asphalt for ballast layer improvement. *International Journal of Integrated Engineering*, *11*(8), pp. 247-258. DOI: https://doi.org/10.30880/ijie.2019.11.08.025

Setiawan, D. M. (2016). Pembatasan kecepatan maksimum dan kaitannya terhadap kapasitas lintas jalur kereta api Muara Enim–Lahat Sumatera Selatan. *Prosiding Seminar Nasional Teknik Sipil ke-VI 2016*, Surakarta, Indonesia. pp. 36-46.

Setiawan, D. M. (2021). Structural response and sensitivity analysis of granular and asphaltic overlayment track considering linear viscoelastic behavior of asphalt. *Journal of the Mechanical Behavior of Materials*, *30*(1), pp. 66-86. DOI: https://doi.org/10.1515/jmbm-2021-0008

Setiawan, D. M. (2022). Subgrade service life and construction cost of ballasted, asphaltic underlayment, and combination rail track design. *Jordan Journal of Civil Engineering*, *16*(1), pp. 173-192.

Setiawan, D. M., Muthohar, I. & Ghataora, G. (2013). Conventional and unconventional railway for rail ways on soft ground in Indonesia (Case study: rantau prapat-duri railways development). *Proceeding of the 16th FSTPT International Symposium*, Universitas Muhammadiyah Surakarta, Surakarta, Indonesia. pp. 610-620.

Setiawan, D. M., Rosyidi, S. A. P. & Budiyantoro, C. (2019). The role of scrap rubber, asphalt and manual compaction against the quality of ballast layer. *Jordan Journal of Civil Engineering*, *13*(4), pp. 594-608.

Shih, J. Y., Thompson, D. & Zervos, A. (2014). Assessment of track-ground coupled vibration induced by high-speed trains. *The 21st International Congress on Sound and Vibration (ICSV21)*. Beijing, China. July 13–17, 2014.

Shih, J. Y., Thompson, D. & Zervos, A. (2016). The effect of boundary conditions, model size and damping models in the finite element modelling of a moving load on a track/ground system. *Soil Dynamics and Earthquake Engineering*, *86*, pp. 12-27. DOI: https://doi.org/10.1016/j.soildyn.2016.07.004

Signes, C. H., Hernandez, P. M., Roca, J. G., del la Torre, M. E. G. & Franco, R. I. (2016). An evaluation of the resilient modulus and permanent deformation of unbound mixtures of granular materials and rubber particles from scrap tyres to be used in subballast layers. *Transportation Research Procedia*, *18*, pp. 384-391. DOI: https://doi.org/10.1016/j.trpro.2016.12.050

Soto, F. M. & Di Mino, G. (2017). Procedure for a temperature-traffic model on rubberized asphalt layers for roads and railways. *Journal of Traffic and Transportation Engineering*, *5*, pp. 171-202. DOI: https://doi.org/10.17265/2328-2142/2017.04.001

Soto, F. M., Di Mino, G. & Acuto, F. (2017). Effect of temperature and traffic on mix-design of bituminous asphalt for railway sub-ballast layer. *10th International Conference on the Bearing Capacity of Roads, Railways and Airfields*. 9 Pages.

Varandas, J. N., Paixão, A., Fortunato, E. & Hölscher, P. (2016). A numerical study on the stress changes in the ballast due to train passages. *Procedia Engineering*, 143, pp. 1169-1176. DOI: https://doi.org/10.1016/j.proeng.2016.06.127

Wang, J. & Zeng, X. (2004). Numerical simulations of vibration attenuation of high-speed train foundations with varied track-bed underlayment materials. *Journal of Vibration and Control*, *10*, pp. 1123-1136. DOI: https://doi.org/10.1177/1077546304043268

Wang, X., Pu, J., Wu, P. & Chen, M. (2020). Modeling of coupling mechanism between ballast bed and track structure of high-speed railway. *Mathematical Problems in Engineering*, 9768904, 12 pages. DOI: https://doi.org/10.1155/2020/9768904

Wehbi, M. & Musgrave, P. (2017). Optimisation of track stiffness on the UK Railways. *The Journal Permanent Way Institution*, *135*(3), pp. 24-31.

Wu, Q., Sun, Y., Spiryagin, M. & Cole, C. (2019). Railway track longitudinal force mode. *International Journal of Vehicle Mechanics and Mobility*, *59*(1), pp. 155-170. DOI: https://doi.org/10.1080/00423114.2019.1673445

Zeng, X. (2005). *Rubber-modified asphalt concrete for high-speed railway road*. Case Western Reserve University Cleveland, Ohio, United States, Final Report for High-Speed Rail IDEA Project 40.